

Fast transport with wall slippage

Zhipeng Tang¹ and Yongbin Zhang*²

¹College of Mechanical Engineering, Changzhou Vocational Institute of Mechatronic Technology, Changzhou, Jiangsu Province, China

²College of Mechanical Engineering, Changzhou University, Changzhou, Jiangsu Province, China

(Received September 26, 2020, Revised February 18, 2021, Accepted February 22, 2021)

Abstract. This paper presents the multiscale calculation results of the very fast volume transport in micro/nano cylindrical tubes with the wall slippage. There simultaneously occurs the adsorbed layer flow and the intermediate continuum fluid flow which are respectively on different scales. The modeled fluid is water and the tube wall is somewhat hydrophobic. The calculation shows that the power loss on the tube no more than 1.0 Watt/m can generate the wall slippage even if the fluid-tube wall interfacial shear strength is 1 MPa; The power loss on the scale 10^4 Watt/m produces the volume flow rate through the tube more than one hundred times higher than the classical hydrodynamic theory calculation even if the fluid-tube wall interfacial shear strength is 1 MPa. When the wall slippage occurs, the volume flow rate through the tube is in direct proportion to the power loss on the tube but in inverse proportion to the fluid-tube wall interfacial shear strength. For low interfacial shear strengths such as no more than 1 kPa, the transport in the tube appears very fast with the magnitude more than 4 orders higher than the classical calculation if the power loss on the tube is on the scale 10^4 Watt/m.

Keywords: adsorbed layer; micro/nano tube; multiscale flow; transport; wall slippage

1. Introduction

The transports of water and some ionic liquids in carbon nanotubes have been found to be unexpectedly fast compared to the classical hydrodynamic theory calculation (Calabrò 2017, Ghoufi *et al.* 2016, Majumder *et al.* 2005, Mattia *et al.* 2014, Whitby and Quirke 2007). It was ascribed to the wall slippage (the low friction), the depletion layer near the wall or both of them (Calabrò *et al.* 2013, Mattia and Calabro 2012). When the channel wall is hydrophobic, the wall slippage easily occurs because of the weak fluid-wall interaction (Liu and Li 2011, Ritos *et al.* 2014, Sofos *et al.* 2015). In a micro/nano slit pore flow, there is a critical power loss on the channel for initiating the wall slippage, and the power loss increase on the channel is just for increasing the interfacial slipping velocity and the flow rate in the channel if the wall slippage occurs (Zhang 2019a). For a low friction slit pore, a small power loss on the channel can generate a large flow rate through the channel unpredicted from the classical flow theory, because of the wall slippage (Zhang 2019a). When the channel wall is hydrophilic, the interfacial slippage was also found (Koklu *et al.* 2017). In this case, the slippage may occur on the solid wall or on the adsorbed layer-fluid interface (Zhang 2019b). In whichever case, the influence of the fluid slippage on the volume transport in the channel is the same as for a hydrophobic wall (Zhang 2019b). When the adsorbed layer-fluid interfacial slippage occurs, the depletion layer can not be used for explaining the over large

flow rate through the channel as the flowing of the adsorbed layer is almost lost in spite of the fluid-wall interaction (Zhang 2019b). The multiscale analysis shows that a narrow slit pore easily results in the interfacial slippage even with a very modest flow rate (Tang and Zhang 2020). The depletion layer near the wall indicating the degrading of the viscosity of the layer may be just the wall slippage. In the case of the wall slippage, it was even imagined that a gaseous layer had been formed on the wall.

However, such an argument was not fully substantiated. There has been the model incorporating both the wall slippage and the depletion layer for explaining the flow enhancement in carbon nanotubes (Mattia and Calabro 2012).

The present paper presents the multiscale calculation results of the dimensional volume flow rate through micro/nano cylindrical tubes when the wall slippage occurs or not. The tube wall is somewhat hydrophobic with the adsorbed layer-tube wall interfacial shear strength widely varying indicating different wall hydrophobicity. Instead of using the slip length model, the interfacial shear strength model was used to describe the wall slippage; Lower the interfacial shear strength, greater the wall slippage. The reason for this model application is that the concept of the slip length should be fictitious, while the wall slippage can be physically explained as the result of the interfacial shear stress exceeding the interfacial shear strength (Zhang 2014). The dimensional critical power loss on the channel was calculated for initiating the wall slippage. The curves of the volume flow rate versus the power loss on the channel were plotted respectively for the assumption of no wall slippage and the wall slippage with different interfacial shear strengths with different channel geometrical values. Import conclusions are drawn concerning the wall slippage

*Corresponding author, Professor
E-mail: engmechl@sina.com

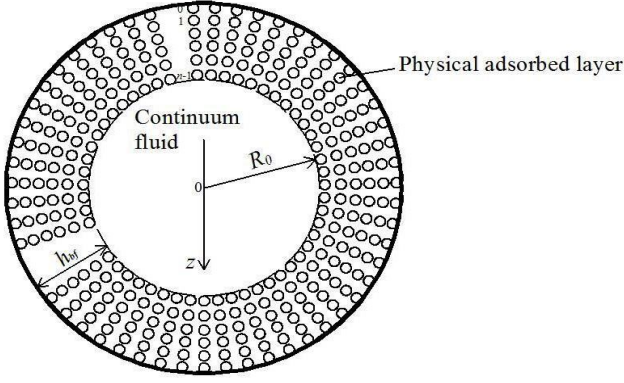


Fig. 1 The studied multiscale transport in micro/nano cylindrical tubes driven by the pressure

influence on the volume transport in micro/nano cylindrical tubes.

2. Multiscale flow in micro/nano cylindrical tubes

Fig. 1 shows the pressure-driven multiscale flow in a micro/nano cylindrical tube where simultaneously occur the adsorbed layer flow and the intermediate continuum fluid flow. The tube inner diameter is so small that it is on the same scale with the thickness h_{bf} of the adsorbed layer. The adsorbed layer flow is essentially non-continuum and molecular-scale governed by the fluid-wall interaction. It is described by the flow factor approach model for nanoscale flow (Zhang 2016). The central continuum fluid flow is described by the Newtonian fluid model. For hydrophobic tube walls, the interfacial slippage may occur on the adsorbed layer-tube wall interface because of the weak adherence of the layer to the tube wall, while it is absent on the adsorbed layer-fluid interface (Zhang 2019a).

3. Analysis

The detailed analysis for the multiscale flow in Fig. 1 considering the wall slippage has been derived in the earlier study (Zhang 2020). The wall slippage is interpreted as the result of the interfacial shear stress exceeding the interfacial shear strength on the adsorbed layer-tube wall interface owing to the pressure gradient. Here are only presented the necessary results.

3.1 Critical power loss on the tube for initiating the wall slippage

The critical power loss on the tube for initiating the wall slippage is (Zhang 2020)

$$POW_{cr} = \frac{K_{cr} \Delta l (\tau_s h_{bf})^2}{\eta} \quad (1)$$

where η is the fluid bulk viscosity, Δl is the axial length of the tube, τ_s is the adsorbed layer-tube wall interfacial shear strength, and

$$K_{cr} = \left[\frac{1}{2\lambda_{bf}(1 + \frac{R_e}{R_0})} \right]^2 \left\{ 2\pi \frac{R_e}{R_0} \left[\frac{4\varepsilon\lambda_{bf}^3}{C_y(1 + \frac{\Delta x}{D})} \left[1 + \frac{1}{2\lambda_{bf}} - \frac{\Delta_{n-2}(q_0 - q_0^n)}{h_{bf}(q_0^{n-1} - q_0^n)} \right] \right. \right. \\ \left. \left. - \frac{2F_1\lambda_{bf}^3}{3C_y} \right] + \frac{\pi}{4} - \frac{4\pi}{C_y} \left[\frac{F_2\lambda_{bf}^2}{6} - \frac{\lambda_{bf}}{1 + \frac{\Delta x}{D}} \left[\frac{1}{2} + \lambda_{bf} - \frac{\Delta_{n-2}(q_0 - q_0^n)}{2R_0(q_0^{n-1} - q_0^n)} \right] \right] \right\} \quad (2)$$

here, $\lambda_{bf} = h_{bf} / (2R_0)$, R_0 is the covering radius of the continuum fluid as shown in Fig. 1, D is the fluid molecule diameter, n is the number of the fluid molecules across the adsorbed layer thickness, R_e is an equivalent constant radius and often $R_e / R_0 = 1 + \lambda_{bf}$, Δx is the separation between the neighboring fluid molecules in the axial direction in the adsorbed layer, $C_y = \eta_{bf}^{eff} / \eta$, η_{bf}^{eff} is the effective viscosity of the adsorbed layer and formulated as $\eta_{bf}^{eff} = Dh_{bf} / [(n-1)(D + \Delta_x)(\Delta_l / \eta_{line,l})_{avr,n-1}]$,

$$\varepsilon = (2DI + II) / [h_{bf}(n-1)(\Delta_l / \eta_{line,l})_{avr,n-1}],$$

$$q_0 = \Delta_{j+1} / \Delta_j, \text{ and } q_0 \text{ is constant,}$$

$$F_1 = \eta_{bf}^{eff} (12D^2\psi + 6D\varphi) / h_{bf}^3,$$

$$F_2 = 6\eta_{bf}^{eff} D(n-1)(\Delta_{l-1} / \eta_{line,l-1})_{avr,n-1} / h_{bf}^2,$$

$$I = \sum_{i=1}^{n-1} i(\Delta_l / \eta_{line,l})_{avr,i},$$

$$II = \sum_{i=0}^{n-2} [i(\Delta_l / \eta_{line,l})_{avr,i} + (i+1)(\Delta_l / \eta_{line,l})_{avr,i+1}] \Delta_i,$$

$$\psi = \sum_{i=1}^{n-1} i(\Delta_{l-1} / \eta_{line,l-1})_{avr,i},$$

$$\varphi = \sum_{i=0}^{n-2} [i(\frac{\Delta_{l-1}}{\eta_{line,l-1}})_{avr,i} + (i+1)(\frac{\Delta_{l-1}}{\eta_{line,l-1}})_{avr,i+1}] \Delta_i,$$

$$i(\Delta_l / \eta_{line,l})_{avr,i} = \sum_{j=1}^i \Delta_{j-1} / \eta_{line,j-1},$$

$$i(\Delta_{l-1} / \eta_{line,l-1})_{avr,i} = \sum_{j=1}^i j \Delta_{j-1} / \eta_{line,j-1}, \quad \eta_{line,j-1} \text{ and } \Delta_{j-1} \text{ are}$$

respectively the local viscosity and the separation between the j^{th} and $(j-1)^{th}$ molecules across the adsorbed layer thickness, and j and $(j-1)$ are respectively the order numbers of the molecules across the adsorbed layer thickness shown in Fig. 1.

3.2 Dimensional volume flow rate through the tube

When the power loss POW on the tube is greater than POW_{cr} , the wall slippage occurs and the dimensional volume flow rate through the tube is (Zhang 2020)

$$q_v = \frac{C_1 POW}{\tau_s}, \text{ for } POW > POW_{cr} \quad (3)$$

where

$$C_1 = \frac{h_{bf}}{\Delta l} \left[1 + \frac{1}{2\lambda_{bf}} - \frac{1 + \frac{\Delta_{n-2}(q_0 - q_0^n)}{D(q_0^{n-1} - q_0^n)}}{2\lambda_{bf} \frac{R_0}{D}} \right] \quad (4)$$

When $POW \leq POW_{cr}$, no wall slippage occurs, and the dimensional volume flow rate through the tube is (Zhang 2020)

$$q_v = C_2 h_{bf}^2 \sqrt{\frac{POW}{\eta \Delta l}}, \text{ for } POW \leq POW_{cr} \quad (5)$$

Where

$$C_2 = \frac{\sqrt{\pi}}{4\lambda_{bf}^2} \left\{ 8 \frac{R_e}{R_0} \frac{\varepsilon \lambda_{bf}^3}{C_y (1 + \frac{\Delta x}{D})} \left[1 + \frac{1}{2\lambda_{bf}} - \frac{\Delta_{n-2}(q_0 - q_0^n)}{h_{bf}(q_0^{n-1} - q_0^n)} \right] - \frac{4R_e F_1 \lambda_{bf}^3}{3R_0 C_y} \right. \\ \left. + \frac{1}{4} - \frac{4}{C_y} \left\{ \frac{F_2 \lambda_{bf}^2}{6} - \frac{\lambda_{bf}}{1 + \frac{\Delta x}{D}} \left[\frac{1}{2} + \lambda_{bf} - \frac{\Delta_{n-2}(q_0 - q_0^n)}{2R_0(q_0^{n-1} - q_0^n)} \right] \right\} \right\}^{1/2} \quad (6)$$

4. Calculation

Calculations were made by taking the fluid as water, which gives $\eta = 0.001 Pa \cdot s$ and $d = 0.28$ nm. The tube length is taken as $\Delta l = 1.0E-6 m$. The tube wall is hydrophobic with a weak interaction with water. The value of the adsorbed layer-tube wall interfacial shear strength τ_s is widely varied to show the influence of different hydrophobicity on the wall slippage and the water transport.

It was taken that $\Delta x / D = \Delta_{n-2} / D = 0.15$ and $\eta_{line,i} / \eta_{line,i+1} = q_0^m$, where q_0 and m are respectively positive constant (Zhang 2020). These input parameter values are close to the real ones.

The parameter C_y is expressed as (Zhang 2020)

$$C_y(H_{bf}) = 0.9507 + \frac{0.0492}{H_{bf}} + \frac{1.6447E - 4}{H_{bf}^2} \quad (7)$$

where $H_{bf} = h_{bf} / h_{cr,bf}$ and $h_{cr,bf}$ is a critical thickness.

The parameters ε , F_1 and F_2 have been respectively regressed out as (Zhang 2020)

$$\varepsilon = 4.56 \times 10^{-6} (\Delta_{n-2} / D + 31.419) (n + 133.8) (q_0 + 0.188) (m + 41.62) \quad (8)$$

$$F_1 = 0.18 (\Delta_{n-2} / D - 1.905) (\ln n - 7.897) \quad (9)$$

and

$$F_2 = -3.707 \times 10^{-4} (\Delta_{n-2} / D - 1.99) (n + 64) (q_0 + 0.19) (m + 42.43) \quad (10)$$

For the weak fluid-tube wall interaction, it was chosen that $m=0.5$, $n=3$, $q_0=1.03$, and $h_{cr,bf}=7$ nm. The input parameter values give that $h_{bf}=1.32$ nm. These input parameter values indicate a kind of hydrophobic tube wall.

5. Results

Fig. 2 shows the values of the dimensional critical power loss POW_{cr} on the tube for initiating the wall slippage for different τ_s and λ_{bf} . Eq. (1) shows that the value of POW_{cr} is in direct proportion to the square of τ_s . For a given λ_{bf} , Fig. 2 shows that the value of POW_{cr} is rapidly reduced with the reduction of τ_s . For high hydrophobicity of the tube wall such as $\tau_s=0.1$ Pa, the critical power loss on the tube for initiating the wall slippage is between $1.0E-14$ Watt/m and $1.0E-17$ Watt/m for $\lambda_{bf}=0.03 \sim 0.5$ (which gives

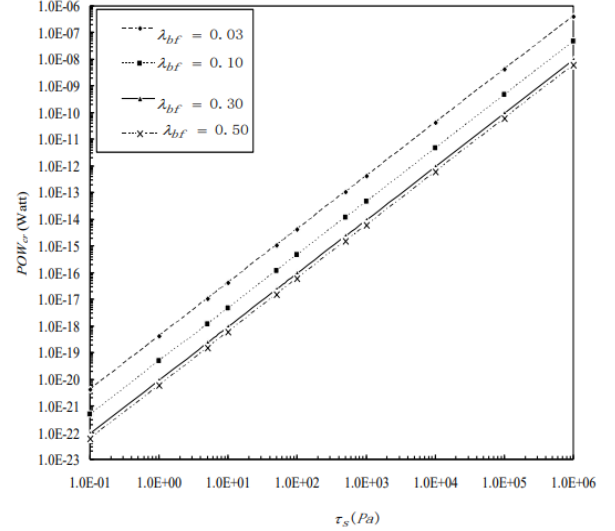


Fig. 2 Dimensional critical power loss on the tube for initiating the wall slippage

the tube inner diameter ranging between 47nm and 5nm). Even for $\tau_s=1$ MPa, the critical power loss for initiating the wall slippage is between 1 Watt/m and 0.01 Watt/m for $\lambda_{bf}=0.03 \sim 0.5$. These results show that the wall slippage is easily generated in micro/nano cylindrical tubes even when the tube wall is hydrophilic. It corresponds to the experimental observation of the wall slippage in a hydrophilic nanotube (Koklu *et al.* 2017). Fig. 2 also shows that for a given τ_s , higher the value of λ_{bf} i.e., smaller the tube inner diameter, lower the value of POW_{cr} . This result matches the analytical and experimental results that narrower the micro/nano cylindrical tube, easier the wall slippage (Tang and Zhang 2020), or greater the slip length (Myers 2017).

Eq. (3) shows that when the wall slippage occurs, the dimensional volume flow rate through the tube is in direct proportion to the power loss on the tube but in inverse proportion to the fluid-tube wall interfacial shear strength τ_s . Fig. 3(a) and (b) show that with the reduction of τ_s i.e., with the increase of the wall hydrophobicity, the dimensional volume flow rate through the tube is rapidly increased. It indicates that the wall slippage plays an important effect. Compared to the results of no wall slippage, the flow rate increase can be 2 to 3 orders for $\tau_s=1$ MPa, 4 to 5 orders for $\tau_s=10$ kPa, 6 to 7 orders for $\tau_s=100$ Pa, and 8 to 9 orders for $\tau_s=1$ Pa. These results qualitatively agree with the experimental findings that the water flow enhancement can be 4 to 5 orders in hydrophobic carbon nanotubes compared to the classical Hagen-Poiseuille equation calculation (Majumder *et al.* 2005, Whitby and Quirke 2007). Fig. 3(a) and (b) also show that when the wall slippage occurs, the volume flow rate through the tube is rapidly increased with the increase of the power loss on the tube. The comparisons between Fig. 3 (a) and (b) show that with the increase of λ_{bf} i.e., with the reduction of the tube inner diameter, the flow enhancement due to the wall slippage is significantly increased. This result also agrees with the molecular dynamics simulation results (Thomas and Mcgaughey 2008).

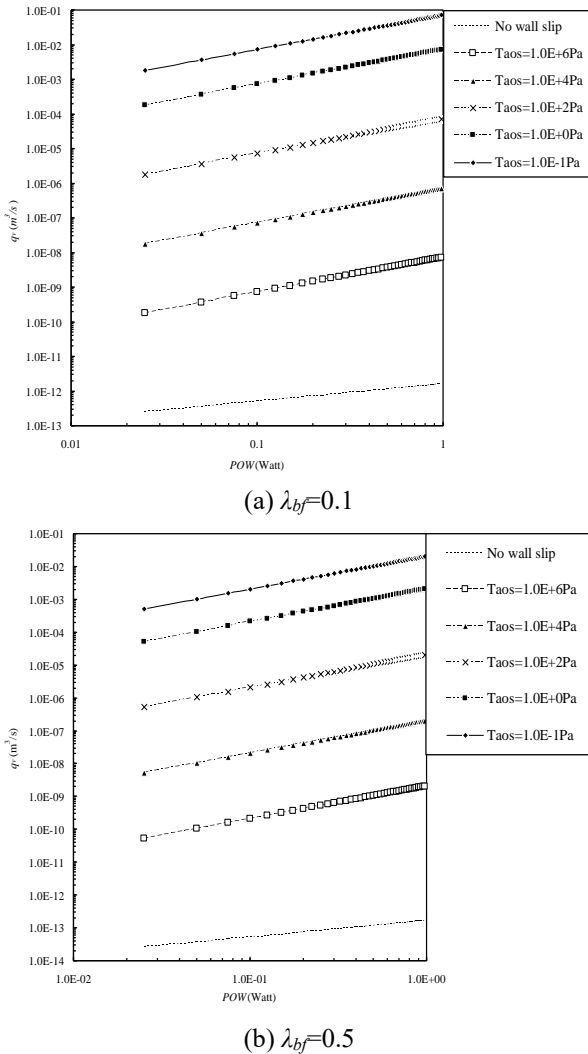


Fig. 3 Dimensional volume flow rates through the tube for different wall hydrophobicity

6. Conclusions

The multiscale calculation results for volume transport in micro/nano cylindrical tubes are presented. The fluid is water, the tube wall is somewhat hydrophobic, and the wall slippage is considered. There is an adsorbed layer on the tube wall, the flow of which is described by the flow factor approach model for nanoscale flow. The central fluid flow in the tube is described by the Newtonian fluid model.

The derived analysis shows that when the wall slippage occurs, the dimensional volume flow rate through the tube is in direct proportion to the power loss on the tube but in inverse proportion to the adsorbed layer-tube wall interfacial shear strength, which depends on the tube wall hydrophobicity. The calculation results show that the wall slippage has a great impact on the transport in the tube and it can heavily increase the flow rate through the tube. The flow enhancement in the tube due to the wall slippage can be 2 to 9 orders depending on the adsorbed layer-tube wall interfacial shear strength τ_s . Lower the value of τ_s , i.e., More hydrophobic the tube wall, greater the flow enhancement. In a narrower micro/nano cylindrical tube, the wall slippage

more easily occurs, and the flow enhancement is more significant. The calculation results qualitatively agree with both the experimental observation and the molecular dynamics simulation results.

References

- Calabrò, F. (2017), "Modeling the effects of material chemistry on water flow enhancement in nanotube membranes", *MRS Bull.*, **42**, 289-293. <https://doi.org/0.1557/mrs.2017.58>.
- Calabrò, F., Lee, K.P. and Mattia, D. (2013), "Modeling flow enhancement in nanochannels: Viscosity and slippage", *Appl. Math. Lett.*, **26**, 991-994. <https://doi.org/10.1016/j.aml.2013.05.004>.
- Ghoufi, A., Szymczyk, A. and Malfreyt, P. (2016), "Ultrafast diffusion of ionic liquids confined in carbon nanotubes", *Sci. Rep.*, **6**, 28518. <https://doi.org/10.1038/srep28518>.
- Koklu, A., Li, J., Sengor, S. and Beskok, A. (2017), "Pressure-driven water flow through hydrophilic alumina nanomembranes", *Microfluid. Nanofluid.*, **21**, 124-135. <https://doi.org/10.1007/s10404-017-1960-1>.
- Liu, C. and Li, Z. (2011), "On the validity of the Navier-Stokes equations for nanoscale liquid flows: The role of channel size", *AIP Adv.*, **1**, 032108. <https://doi.org/10.1063/1.3621858>.
- Majumder, M., Chopra, N., Andrews, R. and Hinds, B. J. (2005), "Enhanced flow in carbon nanotubes", *Nature*, **438**, 44. <https://doi.org/10.1038/438044a>.
- Mattia, D. and Calabro, F. (2012), "Explaining high flow rate of water in carbon nanotubes via solid-liquid molecular interactions", *Microfluid. Nanofluid.*, **13**, 125-130. <https://doi.org/10.1007/s10404-012-0949-z>.
- Mattia, D., Lee, K.P. and Calabro, F. (2014), "Water permeation in carbon nanotube membranes", *Current Opinion Chem. Eng.*, **4**, 32-37. <https://doi.org/10.1016/j.coche.2014.01.006>.
- Myers, T.G. (2011), "Why are slip lengths so large in carbon nanotubes?", *Microfluid. Nanofluid.*, **10**, 1141-1145. <https://doi.org/10.1007/s10404-010-0752-7>.
- Ritos, K., Mattia, D., Calabro, F. and Reese, J. M. (2014), "Flow enhancement in nanotubes of different materials and lengths", *J. Chem. Phys.*, **140**, 014702. <https://doi.org/10.1063/1.4846300>.
- Sofos, F., Karakasidis, T.E. and Liakopoulos, A. (2015), "Fluid structure and system dynamics in nanodevices for water desalination", *Desalin. Water Treat.*, **55**, 1-11. <https://doi.org/10.1080/19443994.2015.1049966>.
- Tang, Z.P. and Zhang, Y.B. (2020), "Critical multiscale flow for interfacial slippage in microchannel", *Front. Heat Mass Transf.*, **14**, 26. <http://dx.doi.org/10.5098/hmt.14.26>.
- Thomas, J.A. and Mcgaughey, A.J.H. (2008), "Reassessing fast water transport through carbon nanotubes", *Nano Lett.*, **8**, 2788-2793. <https://doi.org/10.1021/nl8013617>.
- Whitby, M. and Quirke, N. (2007), "Fluid flow in carbon nanotubes and nanopipes", *Nature Nanotech.*, **2**, 87-94. <https://doi.org/10.1038/nnano.2006.175>.
- Zhang, Y.B. (2014), "Review of hydrodynamic lubrication with interfacial slippage", *J. Balkan Trib. Assoc.*, **20**, 522-538.
- Zhang, Y.B. (2016), "The flow equation for a nanoscale fluid flow", *Int. J. Heat Mass Transf.*, **92**, 1004-1008. <https://doi.org/10.1016/j.ijheatmasstransfer.2015.09.008>.
- Zhang, Y.B. (2019a), "Power loss in multiscale mass transfer", *Front. Heat Mass Transf.*, **13**, 22. <http://dx.doi.org/10.5098/hmt.13.22>.
- Zhang, Y.B. (2019b), "Influence of the fluid-wall interaction on multiscale flow through a micro slit pore considering the adsorbed layer-fluid interfacial slippage", *Front. Heat Mass Transf.*, **13**, 27. <http://dx.doi.org/10.5098/hmt.13.27>.
- Zhang, Y.B. (2020), "Modeling of flow in a micro cylindrical tube

with the adsorbed layer effect: Part II-Results for interfacial slippage”, *Int. J. Heat Mass Transf.* (submitted)

ED